Cellular Oncology (2025) 48:775–787
https://doi.org/10.1007/s13402-025-01048-7

RESEARCH

Thymidine kinase 1 indicates resistance to immune checkpoint plus tyrosine kinase inhibition in renal cell carcinoma

Jiajun Wang[1] · Xianglai Xu[1] · Ying Wang[2] · Yanjun Zhu[1]

Accepted: 12 February 2025 / Published online: 26 February 2025

Abstract

Purpose Immune checkpoint plus tyrosine kinase inhibition (IO + TKI) has emerged as the first-line therapy in metastatic renal cell carcinoma (RCC), but no biomarker can predict its efficacy. Thymidine kinase 1 (TK1) is closely associated with immune evasion in tumors.

Methods Metastatic RCC patients treated by IO + TKI were enrolled from two cohorts (ZS-MRCC, $n = 45$; Javelin-101, $n = 726$). High-risk localized RCC were also enrolled (ZS-HRRCC, $n = 40$). TK1 was assessed by RNA-sequencing in all cohorts, and the immune contexture was assessed by flow cytometry and immunohistochemistry.

Results Higher TK1 expression was found in patients resistant to IO + TKI therapy ($p = 0.025$). High-TK1 group showed poor progression-free survival (PFS) in both the ZS-MRCC cohort ($P = 0.008$) and the Javelin-101 cohort ($P = 0.036$). By multivariate Cox regression, high-TK1 was determined as an independent factor for poor PFS (hazard ratio (HR) = 3.855, $P = 0.002$). High-TK1 expression was associated with decreased granzyme B^+ $CD8^+$ T cells (ρ=-0.22, $P = 0.18$), increased $PD1^+$ $CD4^+$ T cells (ρ = 0.33, $P = 0.04$), increased $PDL1^+$ macrophages (ρ = 0.45, $P < 0.001$), and increased regulatory T cells (ρ = 0.35, $P = 0.03$). A novel random forest (RF) risk score was built by machine learning based on TK1 and immunologic parameters. Combined IO + TKI therapy surpassed sunitinib monotherapy in the low RF risk score group (HR = 0.158, $P < 0.001$), but was inferior to sunitinib in the high RF risk score group (HR, 2.195, $P < 0.001$).

Conclusion High-TK1 expression could be a potential indicator for therapeutic resistance, poor PFS and immune evasion in metastatic RCC under IO + TKI therapy. The novel RF risk score may help stratify patients for IO + TKI therapy.

Keywords Thymidine kinase 1 · Renal cell carcinoma · Immunotherapy · Tyrosine kinase inhibitor · Tumor microenvironment

1 Introduction

Advanced or metastatic renal cell carcinoma (RCC) can lead to relatively poor survival in most patients [1, 2]. Combined immunotherapy (IO) plus tyrosine kinase inhibitor (TKI) have shown superior effect than conventional TKI monotherapy in clinical trials [3–6], and have been recommended by the clinical guideline of RCC [2]. However, even in these landmark clinical trials, a substantial proportion of patients still cannot benefit from IO + TKI therapy, manifested as primary or acquired resistance [3–6]. The lack of available biomarker for IO + TKI therapy still limits precise decision-making in clinic.

Thymidine kinase 1 (TK1) is a key enzyme during DNA precursor synthesis [7]. The presence of TK1 is an important indicator of cell proliferation [7]. TK1 has been applied as a proliferation marker in tumors, together with

Jiajun Wang and Xianglai Xu contributed equally to this work.

✉ Yanjun Zhu
zhu.yanjun@zs-hospital.sh.cn

Jiajun Wang
w.jiajun@hotmail.com

Xianglai Xu
xl.xu@hotmail.com

Ying Wang
wangying920520@163.com

[1] Department of Urology, Zhongshan Hospital, Fudan University, No.180 Fenglin Road, Shanghai 200032, China

[2] Department of Critical Care Medicine, Zhongshan Hospital, Fudan University, Shanghai 200032, China

Ki-67 [8, 9]. Besides, TK1 is also essential for DNA damage repair, as it is essential to the process whereby pools of deoxythymidine triphosphate are generated to replace damaged nucleotides [10, 11]. Therefore, TK1 level was also elevated during tumor therapies related with DNA damage, for example, radiation therapy or chemotherapy [7, 12–14], and TK1 depletion can lead to cell death when exposed to DNA damage [7, 12].

TK1 has been found to be up-regulated in various malignancies such as lung cancer, breast cancer and colorectal cancer, and it could be a potential clinical biomarker for these cancers [15]. Higher level of TK1 was found to be related with poor survival in lung cancer [16, 17]. Interestingly, upregulation of TK1 level was an independent factor for poor prognosis in lung cancer patients receiving immune checkpoint inhibitor (ICI) treatment [18]. Besides, in a preliminary study based on the Cancer Genome Atlas (TCGA) database, elevated TK1 expression was significantly related with unfavorable survival in hepatocellular carcinoma [19]. By single-cell sequencing, TK1 expression was found associated with changes in the tumor microenvironment (TME), especially tumor infiltrating T cells [19]. These reports highlighted the potential role of TK1 in tumor progression, prognosis, and immunotherapy response. However, the role of TK1 in immunotherapy of RCC has not been clarified yet.

In this study, we aimed to evaluate the expression of TK1 in RCC samples and its prognostic relevance under IO + TKI therapy. The correlation between TK1 expression and tumor immune contexture was also part of the research objectives. We further intended to build a predictive model for therapeutic benefit and decision-making between IO + TKI and TKI monotherapy in advanced RCC.

2 Materials and methods

2.1 Study cohorts and datasets

Metastatic RCC patients treated by IO + TKI were enrolled for analysis from two independent cohorts the Zhongshan Hospital metastatic renal cell carcinoma (ZS-MRCC) cohort, and the Javelin-101 cohort.

The ZS-MRCC cohort enrolled 51metastatic RCC patients treated by IO + TKI therapy and without other malignancies. The inclusion criteria for the ZS-MRCC cohort were: metastatic RCC, combined TKI + IO therapy, no history of other malignancy, and available tumor sample. The exclusion criteria were: refusal to participate, unavailable sample, not passing sample quality control, or loss of follow-up (Supplementary Table S1). Six patients were excluded due to sample unavailability or loss of follow-up, so the ZS-MRCC cohort finally included 45 patients. Response to IO + TKI therapy were defined by the Response Evaluation Criteria in Solid Tumors version 1.1 (RECIST 1.1), every 6–8 weeks based on computed tomography [20]. PFS, defined as the time from therapy initiation to disease progression or death, was defined as the primary endpoint. Baseline characteristics of the ZS-MRCC cohort and their correlation with TK1 expression status are listed in Supplementary Table S2.

The Javelin-101 cohort was collected from the Javelin-101 clinical trial [4]. The inclusion criteria for the Javelin-101 cohort were: available tumor sample, previously untreated advanced renal-cell carcinoma with a clear-cell component, at least one measurable lesion according to the RECIST 1.1 criteria, age of 18 years or older, Eastern Cooperative Oncology Group performance-status score of 0 or 1, a fresh or archival tumor specimen, and adequate renal, cardiac, and hepatic function. The exclusion criteria were: active central nervous system metastases, autoimmune disease, current or previous use of glucocorticoids or other immunosuppressants within 7 days before randomization (Supplementary Table S1). The Javelin-101 cohort finally included 726 metastatic RCC patients. Among them, the IO + TKI arm included 354 patients treated by avelumab + axitinib, and the TKI monotherapy arm included 372 patients treated by sunitinib [4]. Patients' baseline characteristics, PFS, transcriptomic and genomic data, were acquired from the previous reports [4, 21]. Supplementary Table S3 shows the baseline characteristics of the Javelin-101 cohort.

For further immunologic and functional studies, the Zhongshan Hospital high risk renal cell carcinoma (ZS-HRRCC) cohort and the Cancer Genome Atlas Clear Cell Kidney Cancer (TCGA-KIRC) dataset were also applied. The ZS-HRRCC cohort included 40 samples of high-risk localized RCC patients. The inclusion criteria for the ZS-HRRCC cohort were: localized or locally-advanced RCC, receiving radical nephrectomy, and no neo-adjuvant therapy (Supplementary Table S1). The exclusion criteria for the ZS-HRRCC cohort were: refusal to participate, not passing sample quality control, or unavailable tumor sample (Supplementary Table S1). Supplementary Table S4 shows the baseline characteristics of the ZS-HRRCC cohort. The TCGA-KIRC dataset is an open-access dataset of 530 clear cell RCC samples, acquired from the UCSC xena browser (https://xena.ucsc.edu/) [22].

The study was approved by the Clinical Research Ethics Committee of Zhongshan Hospital, Fudan University (B2021-119), following the Declaration of Helsinki. Written informed consent was obtained from each participant.

2.2 RNA-sequencing procedures

RNA-sequencing was performed in the ZS-MRCC cohort and the ZS-HRRCC cohort. The MagBeads Total RNA Extraction Kit (Catalog #T02-096) was used for isolation of total RNA. The RNAClean XP Kit (Cat#A63987, Beckman Coulter, Inc. Kraemer Boulevard Brea, CA, USA) and the RNase-Free DNase Set (Cat#79254, QIAGEN, GmBH, Germany) were used for purification of total RNA. The VAHTS Universal V6 RNA-sequencing Library Prep Kit for Illumina (Cat#NR604-02, Vazyme, Nanjing, China) and NovaSeq 6000 equipment (Illumina, USA) were used for RNA library construction and sequencing. For further analysis, read counts were standardized to fragments per kilobase of transcript per million fragments mapped.

2.3 Hematoxylin & eosin (H&E) and immunohistochemistry (IHC) staining

In the ZS-HRRCC cohort, tumor-infiltrating lymphocytes (TILs) were evaluated by H&E staining according to the methodology recommended by the International TILs Working Group [23]. Primary antibodies for IHC markers are listed in Supplementary Table S5. IHC staining was performed in the ZS-HRRCC cohort, according to previously described procedures [24]. Image capture and evaluation was processed by the PANNORAMIC 250 Flash III DX (3DHISTECH Ltd.) and the CaseViewer application (3DHISTECH Ltd.). Evaluation of IHC staining was conducted under six randomized fields for each sample, by three independent investigators blinded to patients' information. The average value was further used for analysis.

2.4 Flow cytometry

In the ZS-HRRCC cohort, fresh RCC tumor samples were collected for flow cytometry analysis, while fresh peripheral blood samples were collected for isolation of white blood cells, which were used as control group of flow cytometry gating strategy. Detailed flow cytometry procedures were previously described [25]. RBC Lysis Buffer (Thermo Fisher Scientific) was used for isolation of white blood cells. Tumor samples were minced after resection, and digested by collagenase IV (Sigma) and DNase I (Sigma). After passing through a 70-μm strainer, tumor samples were treated with RBC lysis buffer (Thermo Fisher Scientific). Samples were then stained with fluorescently labeled membrane marker antibodies after Fc receptors blockade. Intracellular proteins were stained after disposing by Intracellular Fixation & Permeabilization Buffer (Thermo Fisher Scientific). Staining by the fluorochrome-labeled antibodies were performed afterwards, and samples were preserved in cell staining buffer. Flow-cytometry were performed by BD LSRFortessa™ X-20 (BD Biosciences) and analyzed by Flowjo software v10.0 (Tree Star). Primary antibodies for flow cytometry are also listed in Supplementary Table S5.

2.5 Machine learning models for risk stratification

For the construction of machine learning risk models, expression of TK1, CD274, PDCD1, CD8A, GZMK, GZMB and CD4 were included as parameters. Machine learning algorithms used in the study included supervised principal components (SuperPC), survival support vector machine (survivalSVM), stepwise Cox regression (stepCox), Gradient Boosting Machine (GBM) and random forest (RF). The "mixOmics", "survcomp", "superpc", "survivalsvm", "CoxBoost", "plsRcox", "glmnet", "randomForestSRC", and "ggRandomForests" packages of the R software were used for construction of machine learning models. Machine learning procedures were performed on the R software platform (https://www.r-project.org/).

2.6 Statistical analysis

For categorical variables, Chi-square test, Fisher's exact analysis or Cochran-Mantel-Haenszel test were used if appropriate. For continuous variables, Wilcoxon signed-rank test or Kruskal-Wallis H test were used if appropriate. Spearman's correlation test was used for correlation analysis. Kaplan-Meier analysis with log-rank test and Cox regression analysis were used for survival analysis, by the "survival" and "survminer" packages of the R software. The "forestplot", "ComplexHeatmap" and "ggplot2" packages of the R software were used for drawing forest plots and waterfall plots. All statistical analyses were performed by using R software (https://www.r-project.org/). For all stati stical analyses, two-tailed $P<0.05$ was regarded as statistically significant.

3 Results

3.1 High-TK1 expression correlated with progression and poor survival in RCC

Change of TK1 expression during RCC progression was evaluated in the TCGA-KIRC dataset. TK1 expression was upregulated in RCC samples, compared with non-tumor kidney tissues ($P<0.001$, Fig. 1A). TK1 expression was also upregulated in RCC with higher grade (grade 4 vs. grade 1, $P<0.001$; grade 4 vs. grade 2, $P<0.001$; grade 4 vs. grade 3, $P<0.001$; Fig. 1B) and higher stage (stage IV vs. stage I, $P<0.001$; stage IV vs. stage II, $P<0.001$; stage

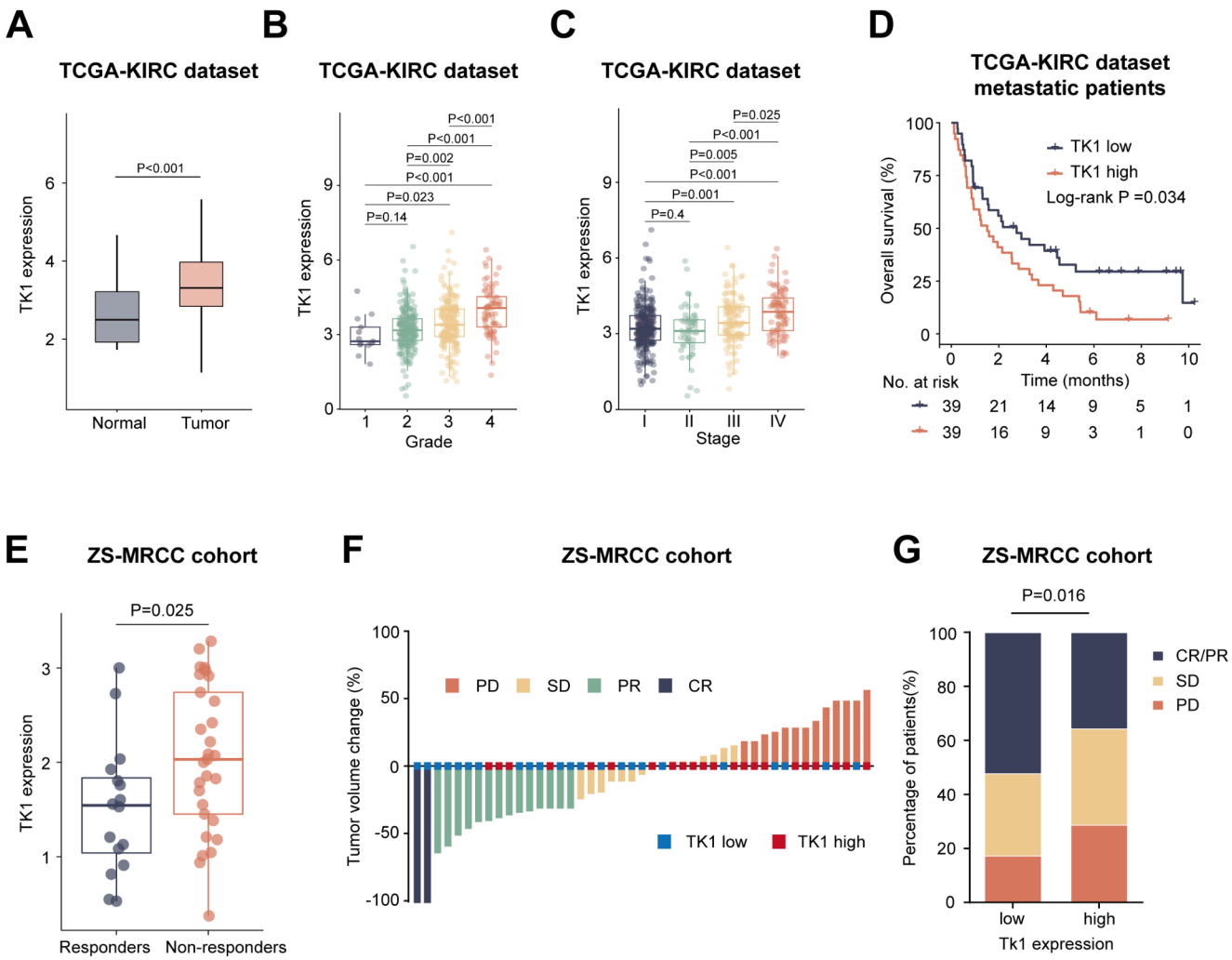

Fig. 1 Overexpression of TK1 is associated with immunotherapy (IO)+tyrosine kinase inhibitor (TKI) resistance in RCC. **A** Elevated TK1 expression in RCC tumor samples. P value, Mann-Whitney U-test. ***, $P<0.001$. **B** & **C** Elevated TK1 expression in RCC with higher TNM stage (**B**) and ISUP grade (**C**). *P* values, Kruskal-Wallis H test. *, $P<0.05$. **, $P<0.01$. ***, $P<0.001$. **D** Elevated TK1 expression indicates poor clinical outcome in metastatic RCC patients. *P* value, log-rank test. **E** Elevated TK1 expression in non-responders of IO+TKI therapy. P value, Mann-Whitney U-test. **F** Percentage of tumor volume change after IO+TKI therapy in the ZS-MRCC cohort. CR, complete response; PR, partial response; SD, stable disease; PD, progressive disease. **G** Therapeutic response of IO+TKI in the ZS-MRCC cohort according to TK1 expression groups divided by the median value. *P* value, Mann-Whitney U-test

IV vs. stage III, $P=0.025$; Fig. 1C). Moreover, metastatic RCC patients with high-TK1 showed poor overall survival ($P=0.034$, Fig. 1D).

3.2 High-TK1 expression correlated with therapeutic resistance of IO + TKI

In the ZS-MRCC cohort of metastatic RCC treated by IO+TKI therapy, high-TK1 expression was elevated in non-responders ($P=0.025$, Fig. 1E). After stratifying patients into high- TK1 and low-TK1 groups according to the median value, the low-TK1 subgroup showed higher rate of CR and PR ($P=0.016$, Fig. 1F and G).

3.3 High-TK1 expression was an independent prognostic factor for poor PFS under IO + TKI therapy

The prognostic role of TK1 expression was evaluated in the ZS-MRCC cohort. In the ZS-MRCC cohort, high-TK1 expression was associated with poor PFS (log-rank $P=0.008$ Fig. 2A). By univariate Cox regression analysis, high-TK1 expression was also correlated with poor PFS (HR=2.773; $P=0.012$, Fig. 2B). Moreover, in a multivariate Cox regression model including tumor histology, IMDC group and TK1 expression, TK1 was identified as an independent prognostic factor for poor PFS (HR=3.855; $P=0.002$, Fig. 2B). Furthermore, The IO+TKI arm of the

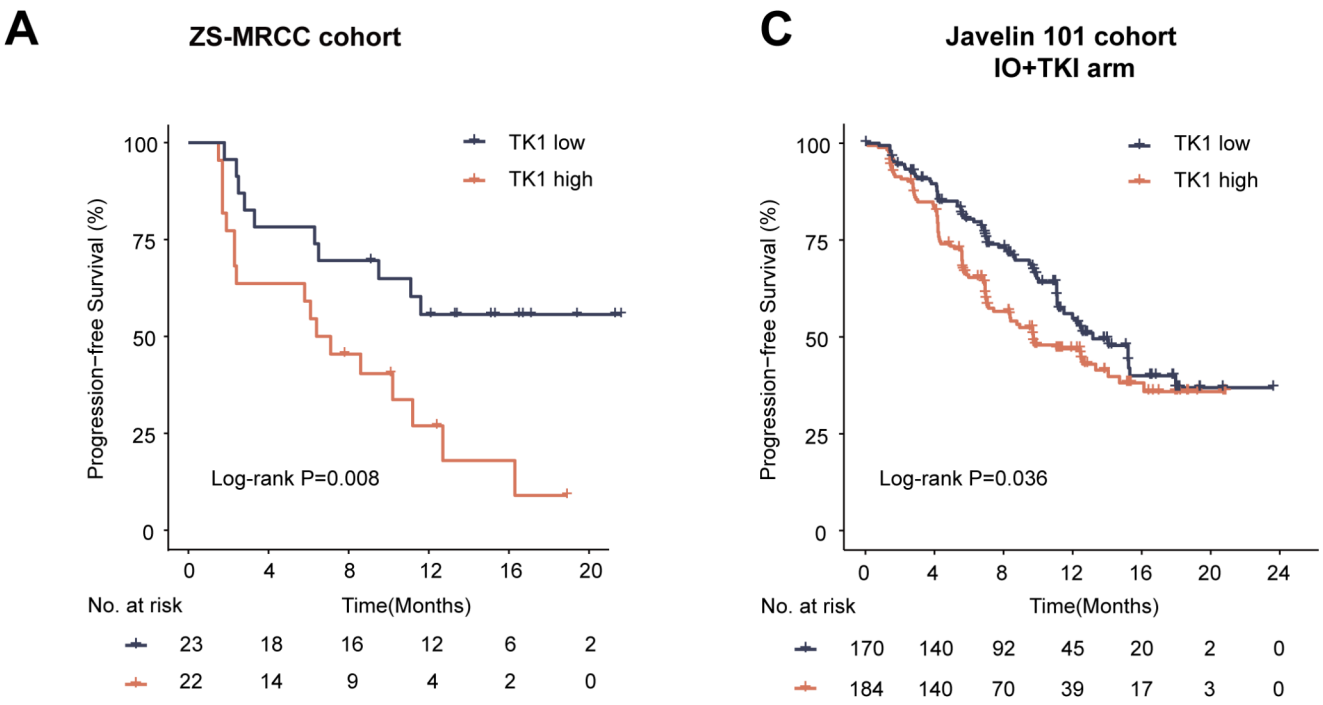

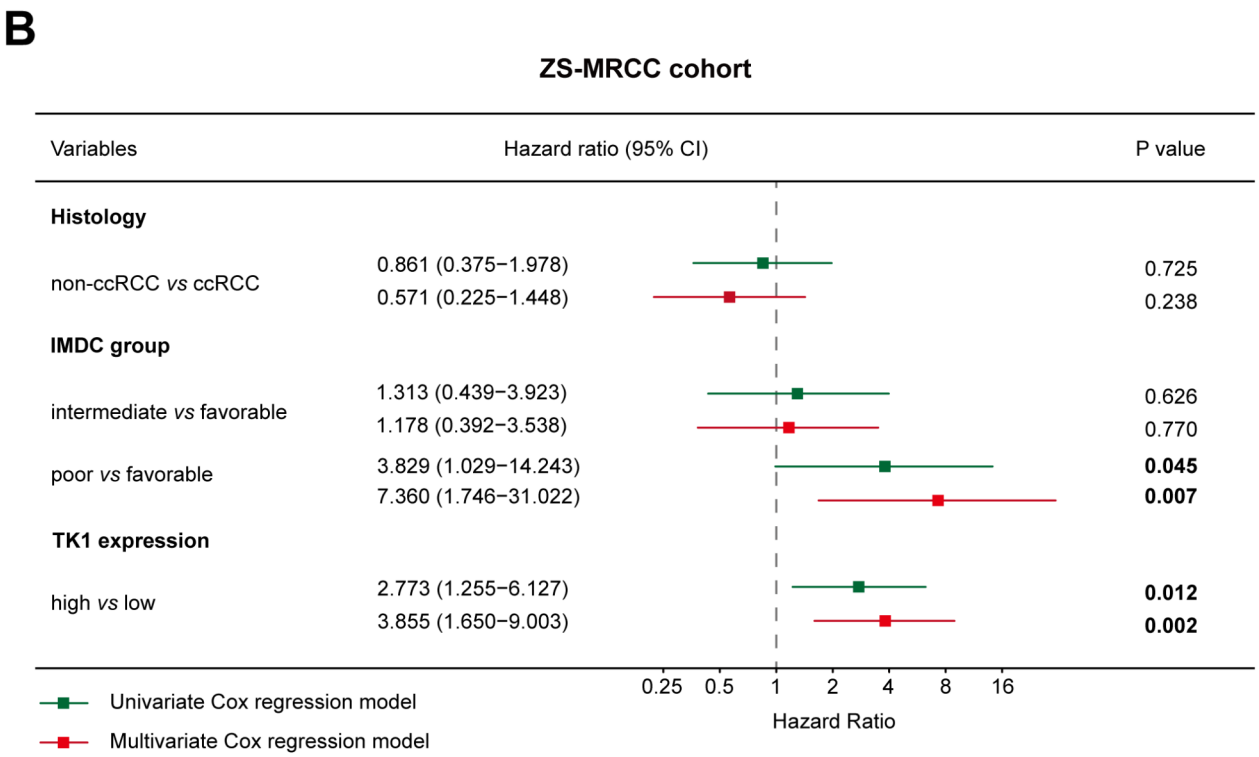

Fig. 2 Overexpression of TK1 is associated with dismal progression-free survival (PFS) in RCC under IO+TKI treatment. **A** PFS in TK1 expression subgroups of the ZS-MRCC cohort. P value, log-rank test. Hazard ratio, univariate Cox regression model. **B** Univariate and multivariate Cox regression models for PFS in the ZS-MRCC cohort. Hazard ratios and P values, Cox regression. **C** PFS in TK1 expression subgroups of the Javelin-101 cohort. *P* value, log-rank test. Hazard ratio, Cox regression analysis

Javelin-101 study was used as external validation cohort. In this cohort, high-TK1 group was also associated with poor PFS by Kaplan-Meier analysis (log-rank $P=0.036$, Fig. 2C).

3.4 Correlation between TK1 expression and T cell abundance in RCC

To identify the correlation between TK1 expression and immune cells in the tumor microenvironment, H&E or IHC staining was performed on RCC specimens (Fig. 3A). TK1 expression did not show significant correlation with $CD8^+$ T cells ($P=0.69$, Fig. 3B) or $CD4^+$ T cells ($P=0.27$, Fig. 3C).

To further evaluate the association between TK1 expression and T cells in RCC, flow cytometry was performed in fresh tissues of RCC (Fig. 3D). Negative correlation was found between TK1 expression and $CD8^+$ T cells (ρ=-0.20, $P=0.22$, Fig. 3E), but showed positive correlation with $CD4^+$ T cells (ρ=0.22, $P=0.16$, Fig. 3F). However, both correlations were not statistically significant.

3.5 Correlation between TK1 expression and T cell function in RCC

Further analyses focused on the function of T cells in RCC. PD1 expression was evaluated in both $CD8^+$ T cells (Fig. 4A) and $CD4^+$ T cells (Fig. 4B). Positive correlations were found between TK1 expression and $PD1^+CD8^+$ T cells (ρ=0.24, $P=0.14$, Fig. 4A), as well as between TK1 expression and $PD1^+CD4^+$ T cells (ρ=0.33, $P=0.04$, Fig. 4B). Meanwhile, negative correlation was found between TK1 expression and $GZMB^+CD8^+$ T cells (ρ= -0.22, $P=0.18$, Fig. 4C).

Expression of immune checkpoints and transcription factors by TILs was further assessed by IHC (Fig. 4D). Positive correlations were found between TK1 expression and TIGIT (ρ=0.25, $P=0.12$), LAG3 (ρ=0.21, $P=0.20$), TCF1 (ρ=0.30, $P=0.06$) and EOMES (ρ=0.24, $P=0.14$) (Fig. 4E).

3.6 Correlation between TK1 expression and immune regulators

Regulatory immune cells were assessed by flow cytometry in RCC samples. No significant correlation was found between TK1 expression and macrophages (ρ=-0.16, $P=0.31$, Fig. 5A). However, positive correlation was found between TK1 expression and $PDL1^+$ macrophages (ρ=0.45, $P<0.001$, Fig. 5B), as well as between TK1 expression and regulatory T cells (ρ=0.35, $P=0.03$, Fig. 5C). Besides, high-TK1 samples showed higher expression of Ki67 by IHC staining ($P<0.001$, Fig. 5D).

Correlation between TK1 expression and immune-regulating cytokines was further assessed in the TCGA-KIRC dataset. Positive correlations were found between TK1 expression and TGF-β (ρ=0.30, $P<0.001$), CXCL8 (ρ=0.33, $P<0.001$), IL10 (ρ=0.13, $P<0.001$) and MMP1 (ρ=0.23, $P<0.001$) expression (Fig. 5E).

3.7 Correlation between TK1 and somatic mutations

Correlation between TK1 and somatic mutations in RCC was assessed in the Javelin-101 cohort (Fig. 5F). High-TK1 tumors showed a higher rate of SETD2 mutations ($P<0.001$), BAP1 mutations ($P<0.001$) and PTEN mutations ($P<0.001$) (Fig. 5F). Besides, high-TK1 samples showed a lower rate of RICTOR mutations ($P<0.001$, Fig. 5F).

3.8 Machine learning models for predicting IO + TKI benefit

To build a predictive model for IO+TKI benefit, different machine learning algorithms were applied, including SuperPC, survivalSVM, StepCox, GBM and RF risk score. Expression of the following genes were used for machine learning model construction: TK1, CD274, PDCD1, CD8A, GZMK, GZMB, CD4. The RF risk score (c-index 0.916, AUC for ROC curve 0.917) outperformed the rest of the models for survival prediction under IO+TKI therapy (Fig. 6A and B). The importance of variables enrolled for the RF risk score were listed in Fig. 6C. For time-dependent survival analysis, the RF risk score still performed well (AUC for 6-months survival: 0.972; AUC for 12-months survival: 0.971; AUC for 18-months survival: 0.973; Fig. 6D).

The median value of the RF risk score was further set as the cutoff for high- and low- RF risk score groups (Fig. 6E). In the low-RF risk score group, IO+TKI surpassed TKI monotherapy ($P<0.001$, HR=0.158, Fig. 6F and H). However, in the high-RF risk score group, the efficacy of the IO+TKI was inferior than that of the TKI monotherapy ($P<0.001$, HR=2.195, Fig. 6G and H). Significant interaction was found between RF risk score groups and IO+TKI benefit (P for interaction<0.001, Fig. 6H). These findings highlighted the possible applicational values of the RF risk score in metastatic RCC.

4 Discussion

Combined IO+TKI regimens have emerged as first-line therapy for RCC recently, according to superior PFS compared with TKI monotherapy in clinical trials [3–6]. However,

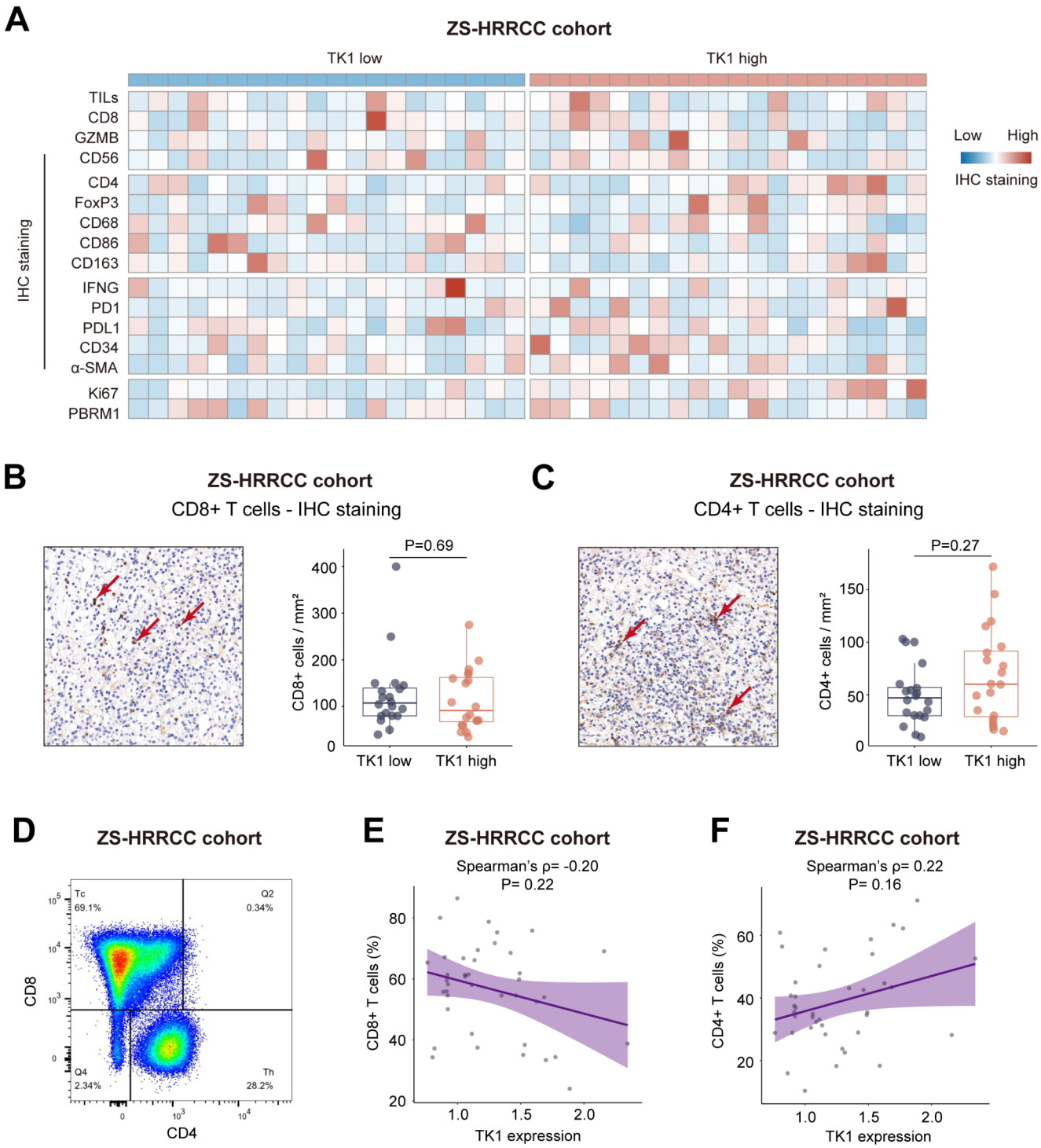

Fig. 3 Relationship between TK1 expression and immune contexture in RCC. **A** Tumor microenvironment contexture in RCC samples ranked by TK1 expression. **B-C** Representative images and quantification of $CD8^+$ T cells (**B**) and $CD4^+$ T cells (**C**) in TK1 expression subgroups. *P* values, Mann-Whitney U-test. **D** Gating strategy for $CD8^+$ T cells and $CD4^+$ T cells by flow cytometry. **E-F** Association between TK1 expression and $CD8^+$ T cells (**E**) and $CD4^+$ T cells (**F**) evaluated by flow cytometry. ρ and *P* values, Spearman's correlation

only part of the patients responds to IO + TKI therapy, as its objective response rate is limited at approximately 20-30% [3–6]. Recent studies are focusing on potential prognostic and predictive biomarkers for immunotherapy in RCC. The BIONIKK study reported a biomarker-based decision-making strategy for RCC immunotherapy, which improved therapeutic benefit of patients [26]. Further studies identified potential prognostic biomarkers for immunotherapy in

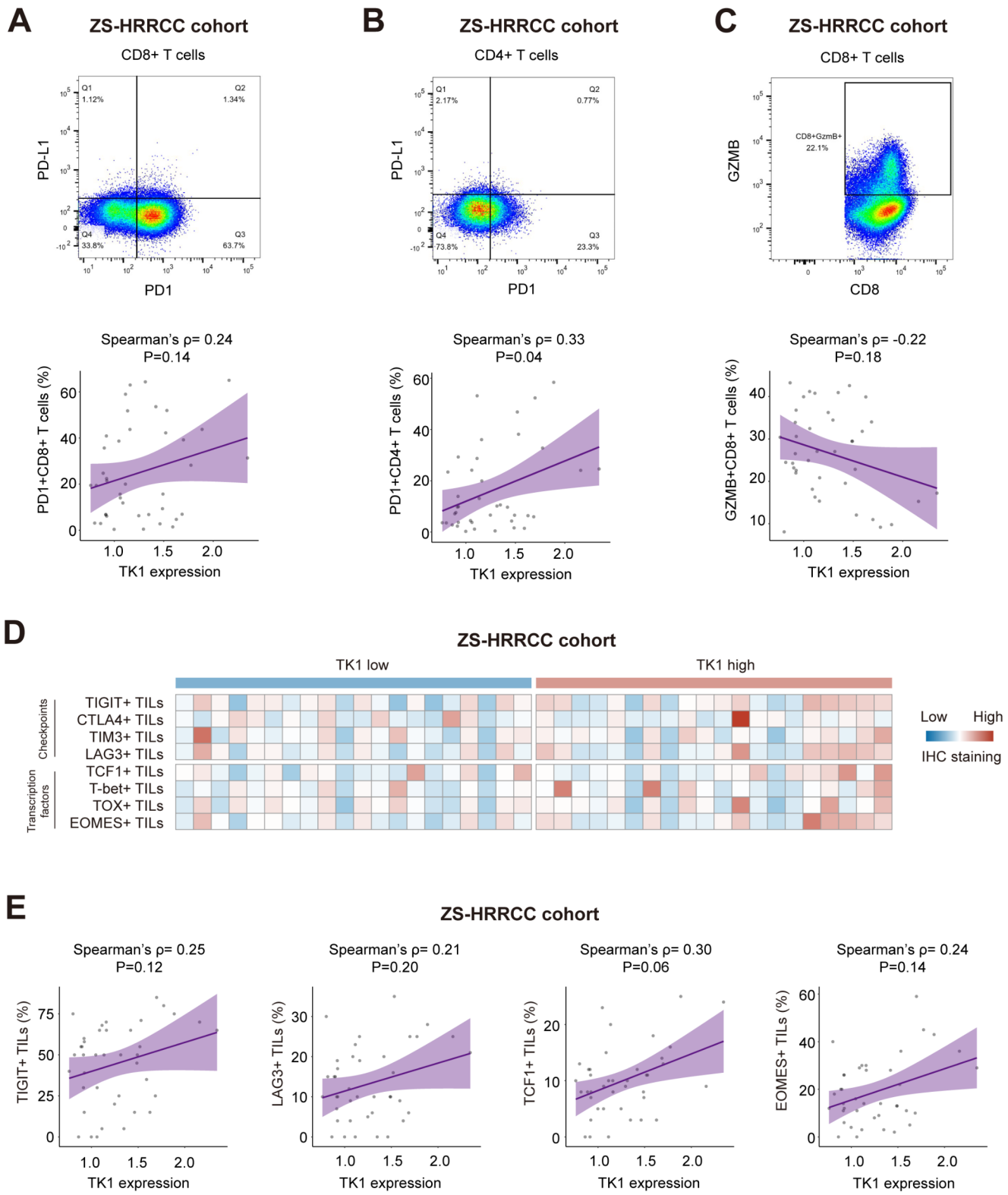

Fig. 4 Exhaustion of T cells related with TK1 overexpression. **A**-**C** Gating strategy for $PD1^{+}CD8^{+}$ T cells (**A**), $PD1^{+}$ $CD4^{+}$ T cells (**B**) and $GZMB^{+}CD8^{+}$ T cells (**C**) by flow cytometry and their correlation with TK1 expression. ρ and P values, Spearman's correlation. **D** Expression of major checkpoints and transcription factors by TILs. **E** Association between TK1 expression and $TIGIT^{+}$ T cells, $LAG3^{+}$ T cells, $TCF1^{+}$ T cells and $EOMES^{+}$ T cells. ρ and *P* values, Spearman's correlation

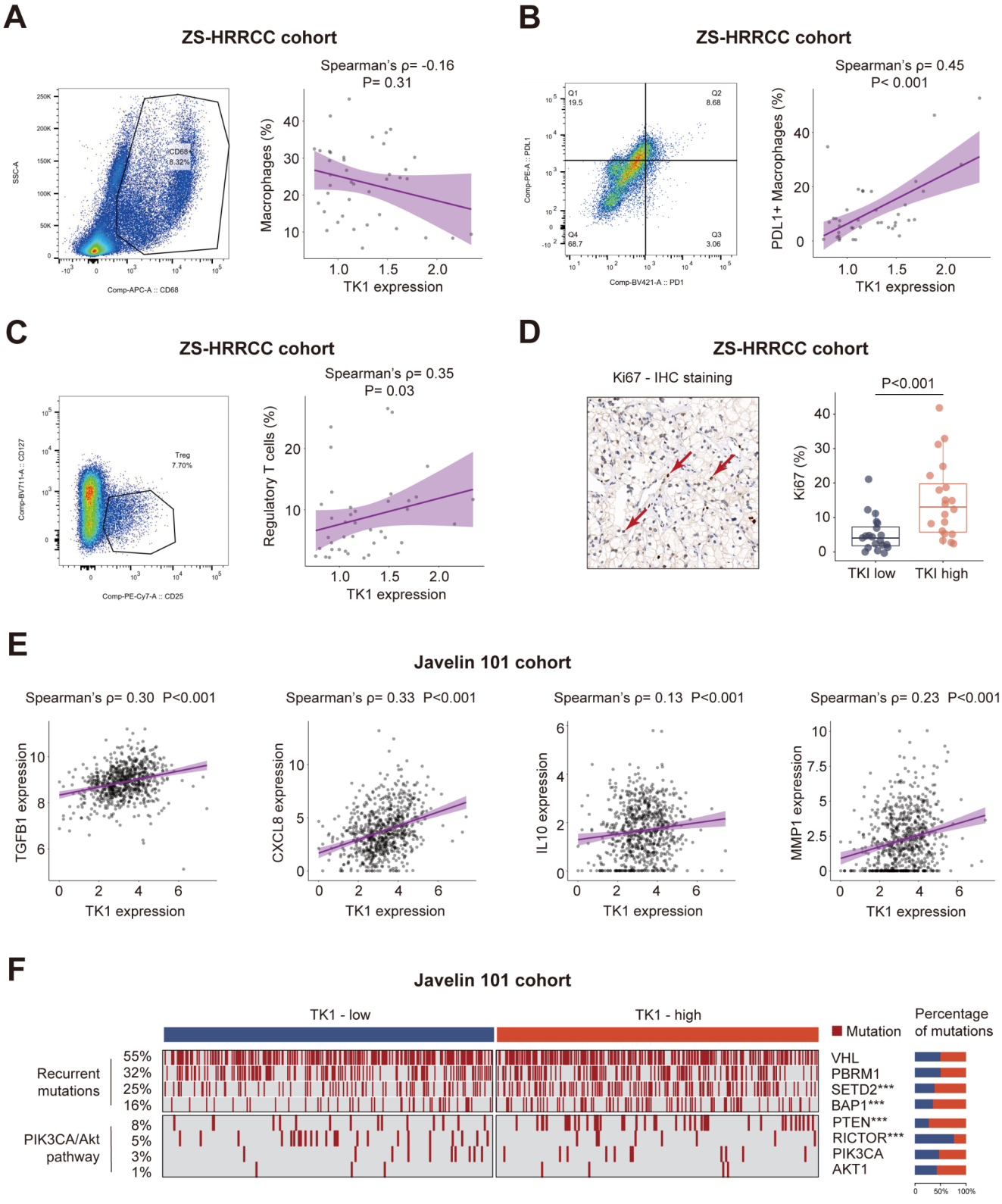

Fig. 5 Overexpression of TK1 is associated with immunosuppressive tumor microenvironment in RCC. **A**-**C** Flow cytometry gating strategy for macrophages (**A**), PDL1+macrophages (**B**) and regulatory T cells (**C**), and their association with TK1 expression. ρ and P values, Spearman's correlation analysis. **D** Quantification of KI67^{+} tumor cells between TK1 expression subgroups by immunohistochemistry. *P* value, Mann-Whitney U-test. **E** Correlation between TK1 and TGFB1, CXCL8, IL10, MMP1 expression in the Javelin-101 cohort. ρ and *P* values, Spearman's correlation. **F** Mutations in the Javelin-101 cohort. Samples ranked by TK1 expression. *P* values, Chi-square test. ***, $P<0.001$

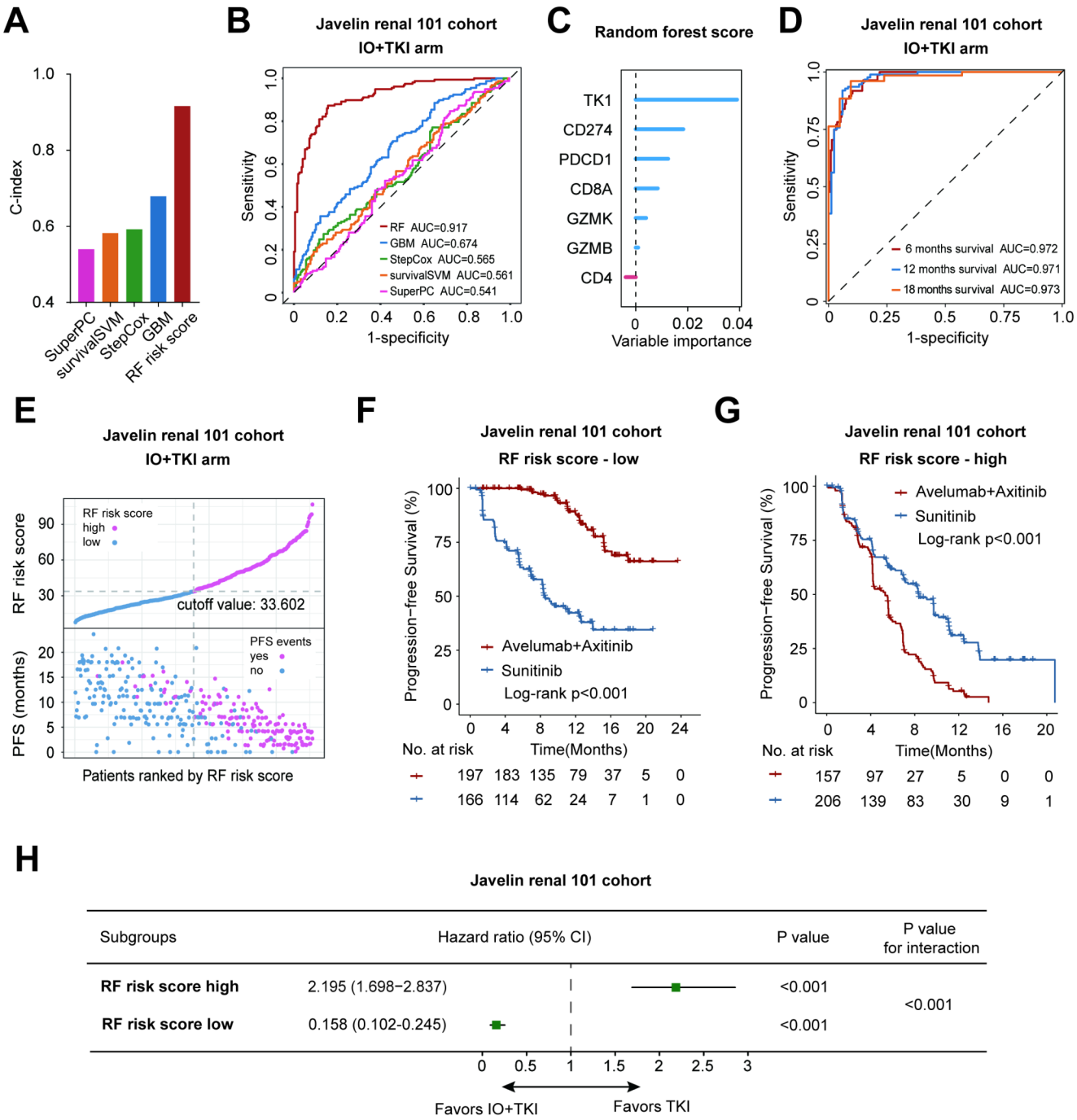

Fig. 6 Machine learning risk scores for prediction of IO+TKI benefit. **A** C-index of different machine learning risk models in the IO+TKI arm of Javelin-101 cohort. SuperPC, supervised principal components; survivalSVM, survival support vector machine; stepCox, stepwise Cox regression; GBM, Gradient Boosting Machine; RF, random forest. **B** Receiver operating characteristic (ROC) curves of tumor progression predicted by machine learning risk models. **C** Genes ranked by variable importance for the random forest (RF) risk score. **D** ROC curves for 6-months, 12-months and 18-months PFS predicted by the RF risk score. **E** Median value set as the cutoff for high/low RF risk score in the IO+TKI arm of Javelin-101 cohort. **F-G** PFS of IO+TKI or TKI in the low RF score group (**F**) and high RF score group (**G**) in the Javelin renal 101 cohort. P values, log-rank test. **H** Survival benefit of IO+TKI versus TKI in the low/high RF risk score subgroups. Hazard ratios and P values, Cox regression test. P for interaction, Cox regression test

clear cell RCC, including TPD52L2 [27], PLAC8 [28], and MYBL1 [29]. However, no biomarker is currently available for IO + TKI combinational therapy in RCC, which limits clinical precision treatment.

As a proliferation biomarker for cancers [7], TK1 was also found related with immunotherapy resistance and TME changes [18, 19]. In this study, high TK1 expression was demonstrated as a biomarker for resistance to IO + TKI therapy (Fig. 1G), and predicted shorter PFS under IO + TKI therapy in two independent cohorts (Fig. 2). More importantly, IO + TKI and TKI monotherapy showed opposite therapeutic benefit in different RF risk score subgroups. In the low-RF risk score group, IO + TKI surpassed TKI monotherapy (Fig. 6F and H). However, in the high-RF risk score group, IO + TKI was inferior to TKI monotherapy (Fig. 6G and H). Significant interaction between RF risk score groups and IO + TKI benefit was further confirmed (P for interaction < 0.001, Fig. 6H). The results may be helpful for clinical decision-making in advanced RCC, since IO + TKI could lead to more immune-related adverse events and more cost. However, due to the limited sample size of the study, further validation studies are still required.

TK1 has also been reported to indicate tumor proliferation and progression [8, 9], and could be up up-regulated in various malignancies, such as lung cancer, breast cancer and colorectal cancer [15]. In our study, TK1 was also upregulated in RCC tumor samples, compared to peritumor samples (Fig. 1A). Moreover, TK1 overexpression was also associated with higher tumor stage and grade in RCC (Fig. 1B and C). These results indicated the potential relevance between TK1 overexpression and tumor progression in RCC. However, the specific mechanisms between TK1 overexpression and RCC progression is still unknown. Nevertheless, since TK1 depletion can lead to cell death when exposed to DNA damage [7, 12], depletion or inhibition of TK1 may still be a viable therapeutic option in RCC.

Literature on the relationship between TK1 expression and the immunosuppressive tumor microenvironment remain scarce. In a preliminary study by single-cell sequencing, TK1 was reported to be significantly associated with the infiltration of B cells, T cells, and dendritic cells in the tumor microenvironment (TME) of hepatocellular carcinoma [19]. TK1 overexpression was also found associated with T cell exhaustion and immunotherapy resistance in lung cancer [18]. These findings highlighted the role of TK1 in tumor immune evasion. In the current study, positive correlation was also observed between TK1 and upregulation of immune checkpoints on T cells (PD1, TIGIT and LAG3, Fig. 4A, B and E). At the same time, transcriptional factors including TCF1 and EOMES were also upregulated on T cells within high-TK1 tumors (Fig. 4E). Since these checkpoints and transcription factors were closely related with T cell dysfunction [30], we implied that T cells may experience exhaustion procedures within high-TK1 tumor TME. Besides, as a major effector for T-cell mediated anti-tumor immunity, GZMB expression was also downregulated within high-TK1 tumors (Fig. 4C). These evidences supported that anti-tumor function of T cells was impaired within high-TK1 tumors.

How TK1 expression induces immune suppression has not been clarified yet. In a recent study by spatial transcriptomics, TK1 overexpression was found closely related with regulatory T cell infiltration [31]. In our study, TK1 was also associated with infiltration of immunosuppressive cells, including $PDL1^{+}$ macrophages and regulatory T cells (Fig. 5B and C). Moreover, TK1 was found associated with immunosuppressive molecules, including TGFB1, CXCL8, IL10 and MMP1 (Fig. 5E). These molecules are important regulators for anti-tumor immunity, and their overexpression can induce immunosuppression [32]. Among them, TGFB1 regulates regulatory T cell differentiation, and induces cytotoxic T cell impairment [33]. TGFB1 also induces monocyte chemotaxis, and affects monocyte-derived macrophage phenotypes [33]. CXCL8 and IL10 are immunosuppressive cytokines released by M2-polarized macrophages and regulatory T cells [34]. MMP1 is an extracellular matrix remodeling enzyme, crucial for immune cell infiltration into the TME [35]. Since TK1 is usually associated with tumor progression and proliferation, TK1 overexpression may also indicate a tumor-promoting microenvironment, with immunosuppression as its main feature. However, the detailed mechanisms of TK1 in tumor immune evasion and IO resistance still need further researches.

The major limitation of the study is its retrospective design and limited sample size. The heterogeneous populations between the ZS-MRCC cohort and Javelin-101 cohort also may lead to selective bias. However, TK1 expression showed association with poor PFS in both cohorts, which demonstrated the robustness of results. Moreover, the different treatment regimens between the ZS-MRCC cohort and Javelin-101 cohort may also interfere with the results. Consequently, further validation studies are still needed. In the study, the RF risk score was found predictive for therapeutic benefit between IO + TKI and TKI in the study. Since IO + IO therapy has also been applied as first-line therapy for metastatic RCC, further studies comparing IO + TKI and IO + IO therapy should also be performed in the future. Besides, the study showed the potential of TK1-targeting therapy in RCC, which also need preclinical studies.

5 Conclusions

Overexpression of TK1 was found associated with T cell exhaustion and immunosuppressive tumor microenvironment in RCC. Overexpression of TK1 indicated resistance to IO+TKI therapy in RCC. The integrated RF risk score could be a novel predictive model for therapeutic benefit and decision-making between IO+TKI and TKI monotherapy in advanced RCC.

Supplementary Information The online version contains supplementary material available at https://doi.org/10.1007/s13402-025-01048-7.

Acknowledgements We are sincerely grateful to all authors and data collectors of the Javelin Renal 101 trial and The Cancer Genome Atlas database for their data sharing.

Author contributions Jiajun Wang and Xianglai Xu conceived and designed the study. Jiajun Wang, Xianglai Xu and Ying Wang contributed to the acquisition, analysis and interpretation of data. Jiajun Wang and Xianglai Xu performed the statistical analysis. Jiajun Wang wrote the manuscript. Xianglai Xu and Yanjun Zhu reviewed the manuscript. Ying Wang and Yanjun Zhu provided technical and material support. Jiajun Wang, Xianglai Xu, Ying Wang and Yanjun Zhu contributed to funding obtaining. Yanjun Zhu contributed to study supervision. All the authors read and approved the manuscript.

Funding This study was funded by grants from National Natural Science Foundation of China (82472795, 82200090, 81902898, 81700660), Natural Science Foundation of Shanghai (24ZR1411000, 19YF1407900), Natural Science Foundation of Fujian Province, China (2024J08348, 2023J05297), Clinical Research Program of Shanghai Municipal Health Commission (20244Y0100), China Urological Oncology Research Fund (H2023-018), and Zhongshan Clinical Research Project (ZSLCYJ202338). All the sponsors have no roles in the study design, in the collection, analysis, or in the interpretation of data.

Data availability No datasets were generated or analysed during the current study.

Declarations

Ethics approval and consent to participate The study followed the Declaration of Helsinki and was approved by the Clinical Research Ethics Committee of Zhongshan Hospital, Fudan University (B2021-119). Informed consent was obtained from each participate.

Competing interests The authors declare no competing interests.

References

1. R.L. Siegel, K.D. Miller, N.S. Wagle, A. Jemal, CA Cancer J. Clin. **73**, 17–48 (2023). https://doi.org/10.3322/caac.21763
2. B. Ljungberg, L. Albiges, Y. Abu-Ghanem, J. Bedke, U. Capitanio, S. Dabestani, S. Fernández-Pello, R.H. Giles, F. Hofmann, M. Hora, T. Klatte, T. Kuusk, T.B. Lam, L. Marconi, T. Powles, R. Tahbaz, A. Volpe, A. Bex, Eur. Urol. **82**, 399–410 (2022). https://doi.org/10.1016/j.eururo.2022.03.006
3. B.I. Rini, E.R. Plimack, V. Stus, R. Gafanov, R. Hawkins, D. Nosov, F. Pouliot, B. Alekseev, D. Soulières, B. Melichar, I. Vynnychenko, A. Kryzhanivska, I. Bondarenko, S.J. Azevedo, D. Borchiellini, C. Szczylik, M. Markus, R.S. McDermott, J. Bedke, S. Tartas, Y.-H. Chang, S. Tamada, Q. Shou, R.F. Perini, M. Chen, M.B. Atkins, T. Powles, N. Engl. J. Med. **380**, 1116–1127 (2019). https://doi.org/10.1056/NEJMoa1816714
4. R.J. Motzer, K. Penkov, J. Haanen, B. Rini, L. Albiges, M.T. Campbell, B. Venugopal, C. Kollmannsberger, S. Negrier, M. Uemura, J.L. Lee, A. Vasiliev, W.H. Miller, H. Gurney, M. Schmidinger, J. Larkin, M.B. Atkins, J. Bedke, B. Alekseev, J. Wang, M. Mariani, P.B. Robbins, A. Chudnovsky, C. Fowst, S. Hariharan, B. Huang, A. di Pietro, T.K. Choueiri, N. Engl. J. Med. **380**, 1103–1115 (2019). https://doi.org/10.1056/NEJMoa1816047
5. T.K. Choueiri, T. Powles, M. Burotto, B. Escudier, M.T. Bourlon, B. Zurawski, V.M. Oyervides Juárez, J.J. Hsieh, U. Basso, A.Y. Shah, C. Suárez, A. Hamzaj, J.C. Goh, C. Barrios, M. Richardet, C. Porta, R. Kowalyszyn, J.P. Feregrino, J. Żołnierek, D. Pook, E.R. Kessler, Y. Tomita, R. Mizuno, J. Bedke, J. Zhang, M.A. Maurer, B. Simsek, F. Ejzykowicz, G.M. Schwab, A.B. Apolo, R.J. Motzer, N. Engl. J. Med. **384**, 829–841 (2021). https://doi.org/10.1056/NEJMoa2026982
6. R. Motzer, B. Alekseev, S.-Y. Rha, C. Porta, M. Eto, T. Powles, V. Grünwald, T.E. Hutson, E. Kopyltsov, M.J. Méndez-Vidal, V. Kozlov, A. Alyasova, S.-H. Hong, A. Kapoor, T. Alonso Gordoa, J.R. Merchan, E. Winquist, P. Maroto, J.C. Goh, M. Kim, H. Gurney, V. Patel, A. Peer, G. Procopio, T. Takagi, B. Melichar, F. Rolland, U. De Giorgi, S. Wong, J. Bedke, M. Schmidinger, C.E. Dutcus, A.D. Smith, L. Dutta, K. Mody, R.F. Perini, D. Xing, T.K. Choueiri, N. Engl. J. Med. **384**, 1289–1300 (2021). https://doi.org/10.1056/NEJMoa2035716
7. K.K. Jagarlamudi, M. Shaw, Biomark. Med. **12**, 1035–1048 (2018). https://doi.org/10.2217/bmm-2018-0157
8. J. Zhou, E. He, S. Skog, Mol. Clin. Oncol. **1**, 18–28 (2013)
9. H. von Euler, S. Eriksson, Vet. Comp. Oncol. **9** (2011). https://doi.org/10.1111/j.1476-5829.2010.00238.x
10. E.E. Bitter, M.H. Townsend, R. Erickson, C. Allen, K L O'Neill Cell. Biosci. **10**, 138 (2020). https://doi.org/10.1186/s13578-020-00493-1
11. Y.-L. Chen, S. Eriksson, Z.-F. Chang, J. Biol. Chem. **285**, 27327–27335 (2010). https://doi.org/10.1074/jbc.M110.137042
12. J. Haveman, J. Sigmond, C. van Bree, N.A. Franken, C. Koedooder, G.J. Peters, Oncol. Rep. **16**, 901–905 (2006)
13. M. Fischer, M. Quaas, L. Steiner, K. Engeland, Nucleic Acids Res. **44**, 164–174 (2016). https://doi.org/10.1093/nar/gkv927
14. K. Engeland, Cell. Death Differ. **25**, 114–132 (2018). https://doi.org/10.1038/cdd.2017.172
15. E.G. Weagel, W. Burrup, R. Kovtun, E.J. Velazquez, A.M. Felsted, M.H. Townsend, Z.E. Ence, E. Suh, S.R. Piccolo, K.S.

Weber, R.A. Robison, and K.L. O'Neill, Cancer Cell Int. **18**, 135 (2018) https://doi.org/10.1186/s12935-018-0633-9
16. X. He, M. Wang, J Oncol **2022**, 8800787 (2022) https://doi.org/10.1155/2022/8800787
17. Y.-T. Wei, Y.-Z. Luo, Z.-Q. Feng, Q.-X. Huang, A.-S. Mo, S.-X. Mo, Biomark. Med. **12**, 403–413 (2018). https://doi.org/10.2217/bmm-2017-0249
18. J. Pan, H. Liu, S. Li, W. Wei, J. Mai, Y. Bian, S. Ning, J. Li, L. Zhang, Heliyon. **9** (2023). https://doi.org/10.1016/j.heliyon.2023.e14129. e14129
19. Q. Cai, M. Zhu, J. Duan, H. Wang, J. Chen, Y. Xiao, Y. Wang, J. Wang, X. Yu, H. Yang, Front. Oncol. **11**, 786873 (2021). https://doi.org/10.3389/fonc.2021.786873
20. E.A. Eisenhauer, P. Therasse, J. Bogaerts, L.H. Schwartz, D. Sargent, R. Ford, J. Dancey, S. Arbuck, S. Gwyther, M. Mooney, L. Rubinstein, L. Shankar, L. Dodd, R. Kaplan, D. Lacombe, J. Verweij, European Journal of Cancer (Oxford, England: 1990) **45**, 228–247 (2009) https://doi.org/10.1016/j.ejca.2008.10.026
21. R.J. Motzer, P.B. Robbins, T. Powles, L. Albiges, J.B. Haanen, J. Larkin, X.J. Mu, K.A. Ching, M. Uemura, S.K. Pal, B. Alekseev, G. Gravis, M.T. Campbell, K. Penkov, J.L. Lee, S. Hariharan, X. Wang, W. Zhang, J. Wang, A. Chudnovsky, A. di Pietro, A.C. Donahue, T.K. Choueiri, Nat. Med. **26**, 1733–1741 (2020). https://doi.org/10.1038/s41591-020-1044-8
22. M.J. Goldman, B. Craft, M. Hastie, K. Repečka, F. McDade, A. Kamath, A. Banerjee, Y. Luo, D. Rogers, A.N. Brooks, J. Zhu, D. Haussler, Nat. Biotechnol. **38**, 675–678 (2020). https://doi.org/10.1038/s41587-020-0546-8
23. S.K. Swisher, Y. Wu, C.A. Castaneda, G.R. Lyons, F. Yang, C. Tapia, X. Wang, S.A.A. Casavilca, R. Bassett, M. Castillo, A. Sahin, E.A. Mittendorf, Ann. Surg. Oncol. **23**, 2242–2248 (2016). https://doi.org/10.1245/s10434-016-5173-8
24. J. Wang, L. Liu, Q. Bai, C. Ou, Y. Xiong, Y. Qu, Z. Wang, Y. Xia, J. Guo, J. Xu, Oncoimmunology. **8**, e1515611 (2019). https://doi.org/10.1080/2162402X.2018.1515611
25. J. Wang, S. Zhang, Y. Wang, Y. Zhu, X. Xu, J. Guo, Urol. Oncol. **41** (2023). https://doi.org/10.1016/j.urolonc.2022.09.009. 51.e13-51.e23
26. Y.-A. Vano, R. Elaidi, M. Bennamoun, C. Chevreau, D. Borchiellini, D. Pannier, D. Maillet, M. Gross-Goupil, C. Tournigand, B. Laguerre, P. Barthélémy, E. Coquan, G. Gravis, N. Houede, M. Cancel, O. Huillard, P. Beuzeboc, L. Fournier, A. Méjean, X. Cathelineau, N. Doumerc, P. Paparel, J.-C. Bernhard, A. de la Taille, K. Bensalah, T. Tricard, T. Waeckel, G. Pignot, E. Braychenko, S. Caruso, C.-M. Sun, V. Verkarre, G. Lacroix, M. Moreira, M. Meylan, A. Bougouïn, L. Phan, C. Thibault-Carpentier, J. Zucman-Rossi, W.H. Fridman, C. Sautès-Fridman and, S. Oudard, Lancet Oncol **23**, 612–624 (2022) https://doi.org/10.1016/S1470-2045(22)00128-0
27. H. Wang, Z. Liu, Y. Du, X. Cheng, S. Gao, Y. Gao, P. Shang, Front. Oncol. **13**, 1210910 (2023). https://doi.org/10.3389/fonc.2023.1210910
28. X. Sun, Z. Liu, Q. Yu, Y. Chen, Y. Sun, Q. Zhu, J. Yang, R. Jiang, Front. Oncol. **13**, 1207551 (2023). https://doi.org/10.3389/fonc.2023.1207551
29. T. Wang, W. Jian, W. Xue, Y. Meng, Z. Xia, Q. Li, S. Xu, Y. Dong, A. Mao, C. Zhang, Front. Immunol. **13**, 1080403 (2022). https://doi.org/10.3389/fimmu.2022.1080403
30. D. Hanahan, O. Michielin, M.J. Pittet, Nat. Rev. Cancer. **25**, 41–58 (2025). https://doi.org/10.1038/s41568-024-00761-z
31. P. Huang, X. Zhou, M. Zheng, Y. Yu, G. Jin, S. Zhang, Front. Immunol. **14**, 1263537 (2023). https://doi.org/10.3389/fimmu.2023.1263537
32. C.T. Kureshi, S.K. Dougan, Cancer Cell. (2024). https://doi.org/10.1016/j.ccell.2024.11.011
33. B.G. Nixon, S. Gao, X. Wang, M.O. Li, Nat. Rev. Immunol. **23**, 346–362 (2023). https://doi.org/10.1038/s41577-022-00796-z
34. C. Engblom, C. Pfirschke, M.J. Pittet, Nat. Rev. Cancer. **16**, 447–462 (2016). https://doi.org/10.1038/nrc.2016.54
35. A. Naba, Nat. Rev. Mol. Cell. Biol. **25**, 865–885 (2024). https://doi.org/10.1038/s41580-024-00767-3